

CRYSTALLIZATION BEHAVIOR OF AMORPHOUS

 $\text{Fe}_{86.38-1.06x}\text{W}_{0.62+0.06x}\text{Si}_3\text{B}_{10+x}$ ALLOYS^①

Hu Wangyu, Zhao Lihua, Yang Qiaoqin, Wang Lingling and Zhang Bangwei

Department of Applied Physics, Hunan University, Changsha 410082, P. R. China

ABSTRACT $\text{Fe}_{86.38-1.06x}\text{W}_{0.62+0.06x}\text{Si}_3\text{B}_{10+x}$ ($x = 0 \sim 22\%$, mole fraction) alloys were prepared by rapid quenching. It was found that the glass-forming range is $15\% \sim 28\%$ B (mole fraction). The experimental results for crystallization temperatures, crystallization phases, heats of crystallization, activation energies and microhardness were presented. The crystallization temperature increases with the increase of microhardness and decreases with the increase of electron concentration. The thermal stability increases first with increasing boron content and decreases later with further increasing boron content, and the most stable case occurs at 23% B (mole fraction).

Key words thermal stability Fe-W-Si-B alloy glass-forming ability microhardness

1 INTRODUCTION

Fe-Si-B alloys have high glass-forming ability (GFA) and practical use as a soft ferromagnetic material. Naka and Masumoto^[1] reported that the formation of the amorphous single phase ranged from 0 to 19% Si (mole fraction) and 10% to 26% B (mole fraction) for the single roller method, Gibson and Delamore^[2] studied the crystallization of the low silicon content Fe-Si-B amorphous alloys, Inoue *et al.*^[3] studied this system with high silicon content and found the glass-forming range was from 0 to 29% Si (mole fraction) and 5% to 26% B (mole fraction), Ramanan^[4] studied the effects on the crystallization behavior due to the addition of a small amount of various elements in the $\text{Fe}_{78}\text{X}_{2}\text{Si}_4\text{B}_{16}$ system ($X = \text{Ti, Zr, Hf, V, Nb, Ta, Cr, Mo, W, Mn, Co, Ni, Pd, Cu, Al}$ and Ge). The ternary Fe-W-B amorphous alloys were also reported in literatures^[5-8]. For the quaternary system, Song *et al.*^[9] had studied the $\text{Fe}_{40}\text{Ni}_{42-x}\text{W}_x\text{B}_{18}$ amorphous alloys.

We had studied the Fe-B binary and Fe-Si-B ternary amorphous alloys^[10-12]. Considering few works on Fe-W-Si-B alloys, in the present

paper we systematically study the glass-forming range, crystallization temperature and crystallization process, heat of crystallization, activation energy and microhardness for the amorphous $\text{Fe}_{86.38-1.06x}\text{W}_{0.62+0.06x}\text{Si}_3\text{B}_{10+x}$ alloys.

2 EXPERIMENTAL

The master ingot was prepared under an argon atmosphere in an arc furnace and its composition was $\text{Fe}_{51.53}\text{W}_{2.59}\text{Si}_{3.93}\text{B}_{41.49}$ (mole fraction, %). Adding iron and silicon to adjust the composition in an induction furnace under an argon atmosphere, the $\text{Fe}_{86.38-1.06x}\text{W}_{0.62+0.06x}\text{Si}_3\text{B}_{10+x}$ ($x = 0, 5, 10, 12, 13, 14, 15, 18, 20$ and 22) alloys were prepared. The alloy buttons, each weighing about 30 g, were remelted several times to ensure the homogeneity of composition. Each alloy buttons were then placed into quartz tubes with a hole of about 0.4 mm in diameter at one end, quickly remelted by induction heating, and then ejected onto a copper chill block of 350 mm diameter rotating at 1500 r/min by pressurized argon gas. The resulting ribbons were about 30 μm in thickness and 1 mm in width.

The crystallization temperatures, heats of

① Received Jan. 3, 1997; accepted May 13, 1997

crystallization, and activation energies for crystallization were studied by means of a calibrated differential scanning calorimeter (DSC), Dupont 1090, in an atmosphere of purified argon and at variable heating rates.

Using $\text{CuK}\alpha$ radiation and a graphite monochromator, X-ray diffraction patterns were employed to check whether ribbons were amorphous and to identify the crystallization products. The microhardness was measured under a load of 0.25 N.

3 RESULTS AND DISCUSSION

The results of X-ray diffraction indicate that the structures of the as-prepared samples are:

- $x = 0$, $\alpha\text{-Fe} + \text{t-Fe}_3\text{B}$;
- $x = 5$, amorphous or $\alpha\text{-Fe} + \text{amorphous}$;
- $x = 10, 12, 13, 14$ and 15 , amorphous;
- $x = 18$, amorphous or $\text{Fe}_2\text{B} + \text{amorphous}$;
- $x = 20$, amorphous + $\alpha\text{-Fe} + \text{Fe}_2\text{B}$;
- $x = 22$, $\alpha\text{-Fe} + \text{Fe}_2\text{B}$.

These results imply that the structures of the ribbons can be divided into three classes. The first class is the easy-forming alloys, which includes the alloys with $x = 10, 12, 13, 14$ and 15 . The second class is the difficult-forming alloys, which includes the alloys with $x = 0, 20$ and 22 , i. e., it is impossible to form amorphous phase in these alloys by rapid quenching. The third class is the critical-forming alloys, which includes the alloys with $x = 5$ and 18 . For these alloys, only operating carefully with desirable spin technical parameters, completely amorphous single phase can be obtained, otherwise, a mixture of amorphous phase and some crystal phase will be obtained. Therefore, for this system, the glass-forming range is from 15% B to 28% B (mole fraction) when the silicon content is at 3% (mole fraction). Naka *et al*^[1] identified the glass-forming range for $\text{Fe}_{100-x}\text{Si}_3\text{B}_x$ ternary system is from 12% B to 22% B (mole fraction) and they predicted the glass-forming range would be from 11% B to 26% B (mole fraction).

These facts show that the GFA is basically not changed by adding tungsten into the Fe-Si-B system, so that tungsten element has similar effects on the GFA as iron element.

Measurements of the crystallization temperatures of amorphous alloys were carried out in the DSC at variable heating rates. The peak crystallization temperature T_p , activation energy E_a and crystallization enthalpy ΔH_c were determined from the DSC measurements and listed in Table 1. The DSC curves for the amorphous alloys show that they only have one exothermic peak except the alloy with $x = 5$. The onset crystallization temperature T_{x0} and peak crystallization temperature T_p at a 10 K/min heating rate are plotted in Fig. 1 as a function of boron content. It is shown that both of them increase rapidly with the increase of boron content at low boron content and decreases a little at high boron content. There is a maximum value at 23% B (mole fraction) and 25B% (mole fraction) for T_{x0} and T_p , respectively.

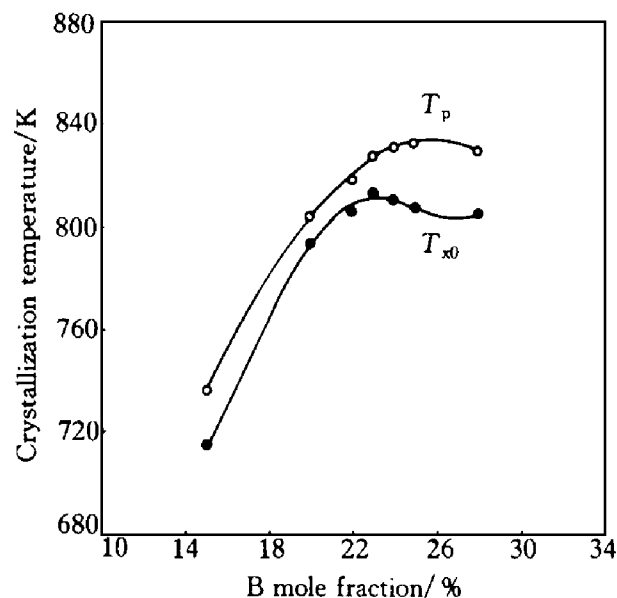


Fig. 1 Onset crystallization temperature T_{x0} and peak temperature T_p against boron content

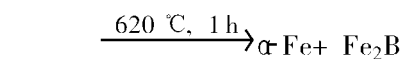
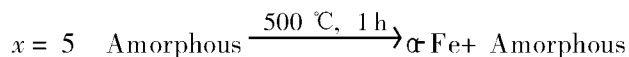
Ramanan^[4] reported that the two peak temperatures were 790.76 K and 812.78 K for $\text{Fe}_{80}\text{Si}_4\text{B}_{16}$ alloy, 741.00 K and 855.00 K for $\text{Fe}_{78}\text{W}_2\text{Si}_4\text{B}_{16}$ alloy at a heating rate of 20 K/min. Hagiwara *et al*^[3] reported the first crystallization temperature for $\text{Fe}_{80}\text{Si}_5\text{B}_{15}$ amorphous wire was 763 K. The two peak temperatures for $\text{Fe}_{81.07}\text{W}_{0.93}\text{Si}_3\text{B}_{15}$ amorphous alloy of the present work are 737 K and 811 K respectively. Gibson and Delamore^[2] reported the peak tem-

Table 1 T_p , E_a and ΔH_c of amorphous $\text{Fe}_{86.38-1.06x}\text{W}_{0.62+0.06x}\text{Si}_3\text{B}_{10+x}$ alloys taken from DSC curves

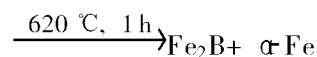
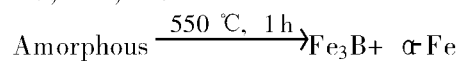
Alloy composition x	Heating rate / $\text{K} \cdot \text{min}^{-1}$	Crystallization temperature / K		Activation energy / $\text{eV} \cdot \text{atom}^{-1}$		Crystallization enthalpy / $\text{kJ} \cdot \text{mol}^{-1}$	
		T_{p1}	T_{p2}	E_{a1}	E_{a2}	ΔH_{c1}	ΔH_{c2}
5	5	724	802	2.36	4.26	3.58	2.92
	10	737	811				
	15	745	816				
	20	750	820				
10	5	795		3.87		6.64	
	10	805					
	15	811					
	20	814					
12	5	808		3.48		6.59	
	10	819					
	15	826					
	20	830					
13	5	819		4.18		5.75	
	10	828					
	15	834					
	20	838					
14	5	821		3.59		8.09	
	10	832					
	15	839					
	20	843					
15	5	821		3.31		7.14	
	10	833					
	15	840					
	20	845					
18	5	818		3.30		6.89	
	10	830					
	15	837					
	20	842					

perature of $\text{Fe}_{74}\text{Si}_4\text{B}_{22}$ alloy was about 823 K, and the peak temperature of $\text{Fe}_{73.64}\text{W}_{1.36}\text{Si}_3\text{B}_{22}$ amorphous alloy in the present work is 819 K.

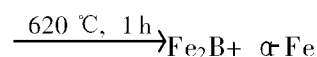
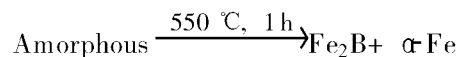
X-ray diffraction studies were performed on all samples after 1 h heat treatment to determine the structures of intermediate and final phases. The results for crystallization processes and products are summarized as follows:



$x = 10, 12, 13 \text{ or } 14$



$x = 15 \text{ or } 18$



For $x = 5$, the crystallization involves two distinct stages as described previously. The first exotherm corresponds to the precipitation of α -Fe, a primary crystallization process. The second exotherm corresponds to the eutectic crystallization process. All the other samples have an eutectic crystallization process, but their crystallization products are different. For $x = 10, 12, 13$ and 14 , the crystallization products are α -Fe and Fe_3B ; for $x = 15$ and 18 , the crystallization products are α -Fe and Fe_2B . At higher temperatures, Fe_3B phase transforms to α -Fe and Fe_2B phases, since Fe_3B phase is a metastable phase.

The enthalpy change upon crystallization, ΔH_c , is determined from the first crystallization DSC peak area at a heating rate of 10 K/min in this work. Fig. 2 shows the compositional dependence of ΔH_c on boron content for the samples measured, which shows a maximum occurs at 24% B (mole fraction). According to other workers^[14, 15], maximum in ΔH_c corresponds to equilibrium or metastable phases, we would expect in the present work this phase is Fe_3B , because the composition of $\text{Fe}_{71.51}\text{W}_{1.49}\text{Si}_3\text{B}_{24}$ is near Fe_3B and its crystallization products indeed have Fe_3B phase, and for higher boron content alloys, the crystallization products are α -Fe and Fe_2B phases.

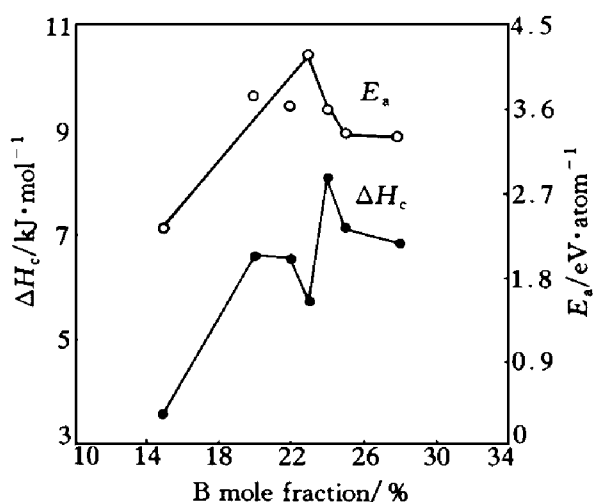


Fig. 2 Enthalpy associated with crystallization ΔH_c and activation energies for crystallization E_a against boron content

There are several ways to determine the ac-

tivation energies for crystallization (E_a)^[16]. The general way is the Kissinger's method with different heating rates. The compositional dependence of E_a for the samples measured is also shown in Fig. 2. E_a increases rapidly with the increase of boron content until it reaches a maximum value at 23% B (mole fraction), then decreases and tends to a definite value with further increasing boron content. This implies that $\text{Fe}_{72.57}\text{W}_{1.43}\text{Si}_3\text{B}_{23}$ alloy is the most stable amorphous alloy.

The correlation between electronic concentration and crystallization temperature is shown in Fig. 3. The average outer-electron concentration increases with the decrease of the crystallization temperature.

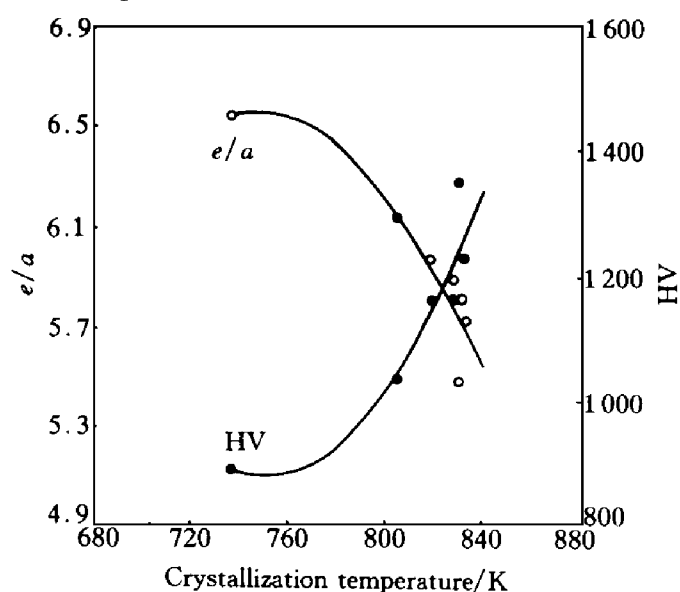


Fig. 3 Average outer electron concentration and microhardness against peak crystallization temperature

There exists a strong correlation between microhardness HV and crystallization temperature for a large number of amorphous alloys^[17]. The higher the HV, the higher the crystallization temperature, and the stronger the thermal stability. Inoue *et al*^[3] identified the similar correlation for the Fe-Si-B amorphous alloys. This correlation for present alloys is also shown in Fig. 3. Indeed, the crystallization temperature increases with the increase of hardness. There are very few data about hardness of Fe-Si-B amorphous alloys with low silicon content.

4 CONCLUSIONS

A series of Fe-W-Si-B alloys have been prepared. The amorphous forming range for the liquid-quenched $\text{Fe}_{86.38-1.06x}\text{W}_{0.62+0.06x}\text{Si}_3\text{B}_{10+x}$ alloys is 15% ~ 28% B (mole fraction).

The crystallization processes of $\text{Fe}_{86.38-1.06x}\text{W}_{0.62+0.06x}\text{Si}_3\text{B}_{10+x}$ amorphous alloys are as follows:

$x = 5$, Amorphous $\longrightarrow \alpha\text{-Fe} + \text{Amorphous}$

$\longrightarrow \alpha\text{-Fe} + \text{Fe}_2\text{B}$;

$x = 10, 12, 13$ and 14 ,

Amorphous $\longrightarrow \text{Fe}_3\text{B} + \alpha\text{-Fe}$

$\longrightarrow \alpha\text{-Fe} + \text{Fe}_2\text{B}$;

$x = 15$ and 18 , Amorphous $\longrightarrow \alpha\text{-Fe} + \text{Fe}_2\text{B}$.

The thermal stability increases first with increasing boron content and decreases later with further increasing boron content, and the most stable case occurs at 23% B (mole fraction).

REFERENCES

- 1 Naka M, Masumoto T. Sci Rep Res Inst Tohoku Univ, 1979, A27: 118.
- 2 Gibson M A, Delamore G W. Mater Sci Eng, 1989, A117: 255.
- 3 Inoue A, Komuro M and Masumoto T. J Mater Sci, 1984, 19: 4125.
- 4 Ramanan V R V. Mater Sci Eng, 1991, A133: 495.
- 5 Nielsen H J V. Phys Status Solidi, 1980, A61: K111.
- 6 Kiss L F, Ashry A, Toth F I and Zambor Balle K. J Magn Magn Mater, 1984, 41: 391.
- 7 Sas B, Kemeny T and Toth J. Solid State Commun, 1986, 59: 195.
- 8 Ganesan K, Narayanasamy A and Nagarajan T. J Phys: Condens Matter, 1990, 2: 4227.
- 9 Song K W, Han K H and Choo W K. Mater Letter, 1992, 13: 387.
- 10 Hu Wangyu and Zhang Bangwei. Physica, 1991, B175: 396.
- 11 Zhang Bangwei, Hu Wangyu and Zhu Deqi. Physica, 1993, B183: 205.
- 12 Wu Lijun, Zhao Lihua, Hu Wangyu, Wang Lingling and Xiao Juemin. Physica, 1994, B193: 116.
- 13 Hagiwara M, Inoue A and Masumoto T. Met Trans, 1982, A13: 373.
- 14 Altounian Z, Tu Guohua and Strom-Olsen J O. J Appl Phys, 1982, 53: 4755; 1983, 54: 3111.
- 15 Mohammed Idrus R and Grundy P J. J Phys D: Appl Phys, 1986, 19: 1245.
- 16 Hu Wangyu, Wu Lijun, Wang Lingling, Zhang Bangwei and Guan Hengrong. Physica, 1994, B203: 147.
- 17 Chen H S. Rep Prog Phys, 1980, 43: 353.

(Edited by Peng Chaoqun)